Available online at www.sciencedirect.com

ScienceDirect

Physics Procedia 70 (2015) 1079 – 1082

Physics Procedia

2015 International Congress on Ultrasonics, 2015 ICU Metz

Nonlinear Echoes from Encapsulated Antibubbles

Kristoffer Johansen[a,b], Spiros Kotopoulis[c], Albert T. Poortinga[d], Michiel Postema[a,*]

[a] *Department of Physics and Technology, University of Bergen, Allégaten 55, 5007 Bergen*
[b] *Institute for Medical Science and Technology, Division of Imaging and Technology, University of Dundee, Dundee DD2 1FD, UK*
[c] *National Centre for Ultrasound in Gastroenterology, Haukeland University Hospital, Jonas Lies vei 65, 5021 Bergen, Norway*
[d] *Department of Mechanical Engineering, Eindhoven University of Technology, 5612 AZ Eindhoven, The Netherlands*

Abstract

An antibubble consists of a liquid droplet, surrounded by a gas, often with an encapsulating shell. Antibubbles of microscopic sizes suspended in fluids are acoustically active in the ultrasonic range. Antibubbles have applications in food processing and guided drug delivery. We study the sound generated from antibubbles, with droplet core sizes in the range of 0–90% of the equilibrium antibubble inner radius. The antibubble resonance frequency, the phase difference of the echo with respect to the incident acoustic pulse, and the presence of higher harmonics are strongly dependent of the core droplet size. Antibubbles oscillate highly nonlinearly around resonance size. This may allow for using antibubbles in clinical diagnostic imaging and targeted drug delivery.

Peer-review under responsibility of the Scientific Committee of ICU 2015
Keywords: Antibubble; Nonlinear; Echo; Rayleigh-Plesset; Targeted drug delivery

1. Introduction

When a bubble is excited by an acoustic pulse, sound is emitted. The sound emitted from individual bubbles adds up to strong nonlinear echoes, which are used in clinical diagnostic imaging to improve contrast between blood and tissue. It has also been shown that bubbles can be used to achieve sonoporation, which is the creation of transient pores in the cell membrane (Kotopoulis et al. (2014)). Hence, when incorporating a droplet, potentially containing a therapeutic agent, into the bubble, as shown in Figure 1A , improved localised drug delivery might be achieved by releasing the droplet core load using acoustics to disrupt the outer gas shell. Bubbles consisting of a liquid core surrounded by gas, often with a thin stabilising shell, are referred to as antibubbles. The radial dynamics of antibubbles is governed by a Rayleigh-Plesset-like equation (Kotopoulis et al. (2015)). Adding an the effect of a finite thickness shell has been proposed by (Johansen et al. (2015)).

This study aims to investigate the singing, *i.e.*, the actual acoustic response, from an antibubble when excited by an acoustic pulse within the clinical ultrasonic frequency range. The radius of the droplet core is varied to illustrate how the sound emitted is dependent on the droplet core size.

* Corresponding author.
E-mail address: Michiel.Postema@ift.uib.no

Peer-review under responsibility of the Scientific Committee of ICU 2015
doi:10.1016/j.phpro.2015.08.230

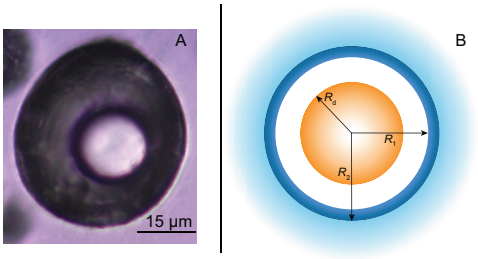

Fig. 1. In A microscopy image of antibubble. In B schematic of a fluid (light blue) containing an antibubble cosisting of a droplet core (orange) of radius R_d, surrounded by a gas layer (white), and thin shell (dark blue) of inner instantaneous radius R_1 and outer instantaneous radius R_2.

2. Theory

Let's consider an antibubble as presented in Figure 1B, where R_1 and R_2 are the respective instantaneous radii of the bubble from the centre of the bubble to the two interfaces, and R_d is the radius of the droplet inside the bubble. As this liquid droplet core can be considered incompressible, R_d is assumed to be constant when the bubble undergoes radial pulsation. The antibubble is surrounded by a shell layer of surface-active material. Both the fluid composing the shell and the outer surrounding liquid are assumed to be viscous and incompressible. Assuming no mass exchange between the respective interfaces, the radial velocity potential $\phi(r,t)$ in the shell and in the surrounding fluid at a distance r from the centre of the bubble can be expressed as (T.G. Leighton (1994)):

$$\phi = -\frac{R_1^2 \dot{R}_1}{r} \,. \tag{1}$$

Conserving radial momentum a Rayleigh-Plesset-like equation is found, like shown in (Johansen et al. (2015); Church (1995))

$$\begin{aligned} &\rho_\mathrm{S} R_1 \ddot{R}_1 \left[1 + \left(\tfrac{\rho_\mathrm{L}-\rho_\mathrm{S}}{\rho_\mathrm{S}}\right)\tfrac{R_1}{R_2}\right] + \rho_\mathrm{S}\dot{R}_1^2\left[\tfrac{3}{2} + \left(\tfrac{\rho_\mathrm{L}-\rho_\mathrm{S}}{\rho_\mathrm{S}}\right)\times\left(\tfrac{4R_2^3-R_1^3}{R_2^3}\right)\right] \\ &= P_\mathrm{g}(R_1,t) - \frac{2\sigma_1}{R_1} - \frac{2\sigma_2}{R_2} - P_0 - P_\mathrm{ac}(t) + 3\int_{R_1}^{R_2}\frac{\tau_{rr}^\mathrm{S}}{r}dr + 3\int_{R_2}^{\infty}\frac{\tau_{rr}^\mathrm{L}}{r}dr \,, \end{aligned} \tag{2}$$

where ρ_S is the density of the shell, ρ_L is the density of the surrounding liquid, $P_\mathrm{g}(R_1,t)$ is the gas pressure inside the antibubble, σ_1 and σ_2 are the surface tension for interface 1 and 2, respectively, P_0 is the ambient pressure, $P_\mathrm{ac}(t)$ is the driving pressure, τ_{rr}^S and τ_{rr}^L is the radial stress in the shell and the surrounding fluid respectively.

Let us assume a pressure change in the surrounding fluid under adiabatic conditions inside the bubble

$$p_{\mathrm{g}0} V_0^\gamma = p_\mathrm{g} V^\gamma \,, \tag{3}$$

where $p_{\mathrm{g}0}$ is the initial gas pressure, V_0 is the initial volume of the gas, γ is the polytropic exponent of the gas, p_g is the instantaneous gas pressure, and V is the instantaneous gas volume. From Figure 1B it is evident that the instantaneous pressure inside the antibubble can be expressed as

$$p_\mathrm{g} = p_{\mathrm{g}0}\left(\frac{R_{10}^3 - R_\mathrm{d}^3}{R_1^3 - R_\mathrm{d}^3}\right)^\gamma \,. \tag{4}$$

Substituting (4) for the gas pressure inside the antibubble, and computing the two last integrals, knowing that $\tau_{rr} = 2\eta(\partial u/\partial r)$ is the shear viscous stress in a Newtonian fluid, a Rayleigh-Plesset-like equation for an antibubble with a Newtonian shell of finite thickness surrounded by a Newtonian viscous liquid can be found:

$$\rho_S R_1 \ddot{R}_1 \left[1 + \left(\frac{\rho_L - \rho_S}{\rho_S}\right)\frac{R_1}{R_2}\right] + \rho_S \dot{R}_1^2 \left[\frac{3}{2} + \left(\frac{\rho_L - \rho_S}{\rho_S}\right) \times \left(\frac{4R_2^3 - R_1^3}{R_2^3}\right)\right] = p_{g0}\left(\frac{R_{10}^3 - R_d^3}{R_1^3 - R_d^3}\right)^{\gamma} - \frac{2\sigma_1}{R_1} - \frac{2\sigma_2}{R_2} - P_0$$
$$-4\eta_L \frac{R_1^2}{R_2^3}\dot{R}_1 - 4\eta_S \frac{(R_2^3 - R_1^3)}{R_1 R_2^3}\dot{R}_1 - P_{ac}(t)\,, \tag{5}$$

where η_L and η_S are the shear viscosity in the liquid and the shell, respectively. From (5) it can be seen from the first term on the left-hand side that the acceleration increases if $\rho_L > \rho_S$, and the acceleration decreases if $\rho_L < \rho_S$. The ratios of the densities effects the second term on the left-hand side in a similar way, decreasing and increasing the degree of nonlinearity. The first term on the right-hand side is a different form of a Rayleigh-Plesset-like equation, describing the radial pulsation of a gas bubble. With a relatively large core droplet size, the pressure inside an antibubble will be larger than in a gas bubble under the same conditions. This makes it possible to predict that antibubbles should have a larger maximum excursion, and a different frequency-content in the oscillations compared to a gas bubble with no load.

For a small excursion ξ of an antibubble, an analytic solution exists if $R_0\xi$ is small. Assuming $R = R_0(1+\xi)$, where $\xi \ll 1$, the damped resonance frequency to (5) is found:

$$\omega_d^2 = \frac{1}{\alpha\rho_S R_{10}^2}\left\{\frac{3\gamma p_{g0}}{1 - \left(\frac{R_d}{R_0}\right)^3} - \frac{2\sigma_1}{R_{10}} - \frac{2\sigma_2 R_{10}^3}{R_{20}^4} - 4\frac{\eta_L^2 R_{10}^4}{\alpha\rho_S R_{20}^6} - 4\frac{\eta_S^2 (R_{20}^3 - R_{10}^3)^2}{\alpha\rho_S R_{10}^2 R_{20}^6}\right\}. \tag{6}$$

It can be observed that increasing the respective viscosities decreases the damped resonance frequencies (Johansen et al. (2015)).

Theoretical prediction of echoes from bubbles have both been computed for compressible and incompressible surrounding fluids, however the difference is insignificant. The scattered echo can then be expressed as (Morgan et al. (2000)):

$$P_e = -\rho_L \dot{\phi} = \rho_L \frac{R_1^2 \ddot{R}_1 + 2R_1 \dot{R}_1^{\,2}}{r}\,. \tag{7}$$

Computations were performed using the ode45 Runga-Kutta algorithm in MATLAB® 2014a (The Mathworks, Inc., Natick, MA, USA). The following fixed parameters were used: $P_0 = 1$ atm, $\gamma = 1.4$, $\eta_L = 1.0$ mPa s, $\eta_S = 1.0$ Pa s, $\rho_S = 1100\,\mathrm{kg/m^3}$, $\rho_L = 998\,\mathrm{kg/m^3}$, $\sigma_1 = 0.051$ N/m, $\sigma_2 = 0.072$ N/m, and $R_2 - R_1 = 2$ nm. Frequency spectra of the radius-time curves were computed using the FFT algorithm in MATLAB®.

3. Results and Discussion

Figure 2 shows an overview of generated echoes of all simulations at MI=0.1 for antibubbles with a Newtonian shell. To clarify how to interpret Figure 2A cross sections were added, B and C, simulated at 40% and 80% core droplet radius, respectively. Analogously, in the frequency spectrogram shown in Figure 2D, cross sections were added at the same core droplet radii. From Figure 2A it can be seen, that the phase of the generated echoes to the antibubble with respect to the incident sound wave is dependent of the core droplet radius, as observed in Figure 2A. Around resonant size, when the antibubbles undergo inertial growth and collapse the strongest echoes are generated. This can be observed from the narrow red bands interlaced with wide blue bands.

At smaller core droplet radii, a more linear echo regime is observed, as depicted by the equal thickness bands. At ~70% core droplet radius, phase changes can be seen after 2 cycles. From Figure 2E and Figure 2F it can be appreciated that antibubbles both with a 40% and 80% core droplet radius have higher harmonics in the generated echo because of the nonlinear response. Around 80% core droplet radius, strong higher harmonics can be observed in the spectrogram of Figure 2D, whereas at core droplet sizes much less, the nonlinear content is limited to the second harmonic, and of significant lower amplitude.

Studying Figure 2B and Figure 2C it can be observed that the antibubble excited close to resonance generates an echo which is a factor of 3 times greater than the antibubble which is excited far away form resonance. Comparing the magnitude of the second harmonics in Figure 2E and Figure 2F the antibubble with a 80% core droplet size has a 12 dB higher second harmonic component, showing that is is important that bubbles are excited around resonance size if they should be applied in clinical diagnostic imaging.

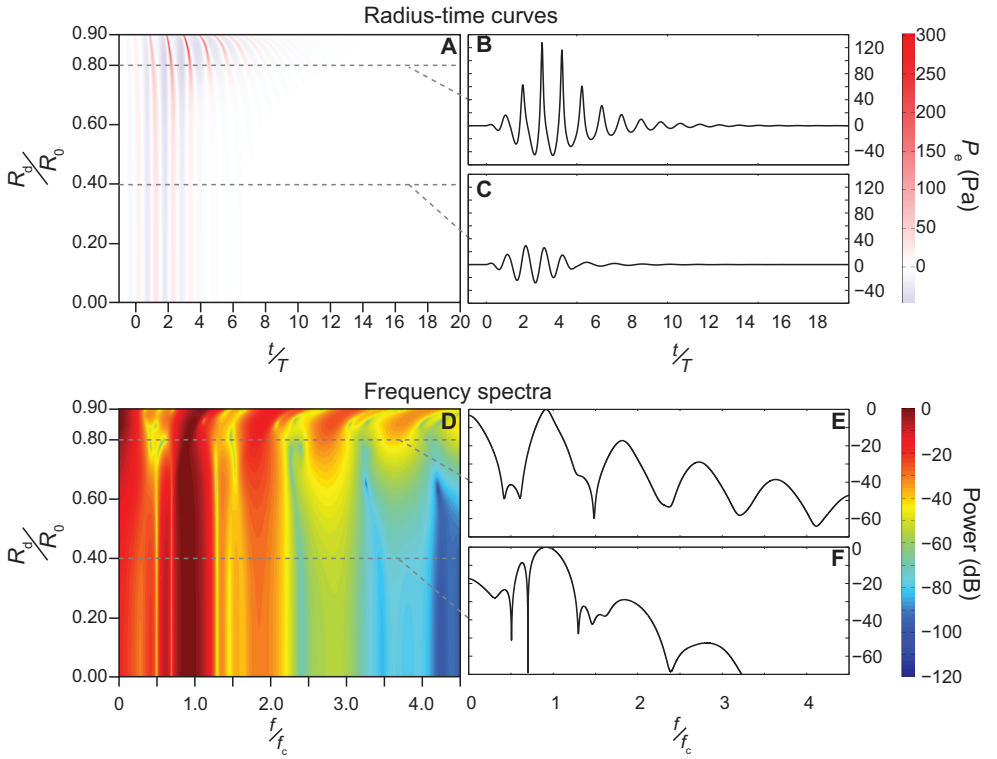

Fig. 2. Scattered echo curves for an antibubble with a Newtonian viscous shell as a function of core droplet radius and sonication time in A with respective cross sections, B and C; radius-time curves in A have been transformed to frequency spectra in D, creating a spectrogram of instantaneous antibubble radius as a function of core droplet radius with respective cross sections, E and F. The MI=0.1. Echoes are computed at a distance $r = 0.01$ m for the respective bubbles. Bubble radii have been normalised to the equilibrium radius $R_0 = 2.5\,\mu$m; core droplet radii have been normalised to equilibrium radius; time has been normalised to the period of the transmitted ultrasound; frequencies have been normalised to the centre frequency of the transmit pulse.

4. Conclusion

The damped resonance frequency, the radial pulsations, and the generated echo from an antibubble are all strongly dependent on core droplet size. Owing to the presence of a droplet core, oscillations are highly nonlinear, and the generated echo contains strong higher harmonics allowing for harmonic imaging methods.

References

Church, C.C., 1995. The effects of an elastic solid surface layer on the radial pulsations of gas bubbles. J. Acoust. Soc. Am. 97, 1510–1521.

Johansen, K., Kotopoulis, S., Postema, M., 2015. Ultrasonically driven antibubbles encapsulated by Newtonian fluids for active leakage detection. Lecture Notes in Engineering and Computer Science: Proceedings of The International MultiConference of Engineers and Computer Scientists 2015 , 750–754.

Kotopoulis, S., Delalande, A., Popa, M., Mamaeva, V., Dimcevski, G., Gilja, O.H., Postema, M., Gjertsen, B.T., Mc Cormack, E., 2014. Sonoporation-enhanced chemotherapy significantly reduces primary tumour burden in an orthotopic pancreatic cancer xenograft. Mol. Imaging Biol. 16, 53–62.

Kotopoulis, S., Johansen, K., Gilja, O.H., Poortinga, A.T., Postema, M., 2015. Acoustically Active Antibubbles. Acta Physica Polonica A 127, 1115–1118.

Morgan, K.E., Allen, J.S., Dayton, P.A., Chomas, J.E., Klibanov, A. L. Ferrara, K.W., 2000. Experimental and theoretical evaluation of microbubble behavior: effect of transmitted phase and bubble size. IEEE Trans. Ultrason. Ferroelectr. Freq. Control. 47, 1494–1508.

T.G. Leighton, 1994. The Acoustic Bubble. Academic Press, London.